

1    **Kinetic and Thermodynamic Control in Dynamic Covalent Synthesis**

2    Andrew J. Greenlee,<sup>†,‡</sup> Chloe I. Wendell,<sup>†,‡</sup> Morgan M. Cencer,<sup>‡</sup> Summer D. Laffoon,<sup>‡</sup> Jeffrey S.  
3    Moore <sup>\*,‡,§</sup>

4    <sup>‡</sup>Department of Chemistry, University of Illinois at Urbana–Champaign, 600 S Mathews Ave,  
5    Urbana, Illinois 61801, United States

6    <sup>#</sup>Beckman Institute for Advanced Science and Technology, University of Illinois at Urbana–  
7    Champaign, 405 N Mathews Ave, Urbana, Illinois 61801

8    **Keywords:** dynamic; covalent; reversible; kinetic; thermodynamic

9    **Abstract** In recent years, dynamic covalent chemistry (DCC) has seen the synthesis of  
10    increasingly complex cyclooligomers, polymers, and diverse compound libraries. The reversible  
11    formation of covalent bonds characteristic of DCC reactions favors thermodynamic product  
12    distributions for simple unitopic reactions; however, kinetic effects are increasingly influential in  
13    reactions of multitopic precursors. In this review, we explore the interplay between  
14    thermodynamic and kinetic considerations when planning a DCC synthesis. Computational  
15    models, typically based on reaction thermodynamics, have aided in predicting DCC reaction  
16    outcomes with moderate success. A clear direction for the field is to develop more robust  
17    computational tools informed by thermodynamic and kinetic driving forces that can predict  
18    product distributions in DCC reactions.

19

20    **Dynamic covalent chemistry (DCC)** is an efficient synthetic strategy that utilizes  
21    **multitopic** precursors designed to form **reversible** covalent bonds, combining advantages of **error**  
22    **correction** during synthesis with the stability of a covalent compound as the final product. It has  
23    enabled the synthesis of a variety of molecular architectures, often isolated as a single, discrete  
24    species, including macrocycles [1], cages [2], and covalent organic frameworks [3,4]. A literature  
25    survey on 1,100 papers acquired through a search of the term “dynamic covalent” indicates that  
26    polymers are the most common target, followed by cages, macrocycles, and COFs [5]. Reversible  
27    bonds commonly in use include imine, boronic ester, hydrazine, disulfide, alkyne, oxime and  
28    alkene exchange, listed in order of their frequency. These structures have found applications in

29 host-guest chemistry [6], organic electronic materials [7], information storage and retrieval [8],  
30 catalysis [9], biological applications [10], chemical sensing [11], and as building blocks for other  
31 materials, such as nanofibers [12].

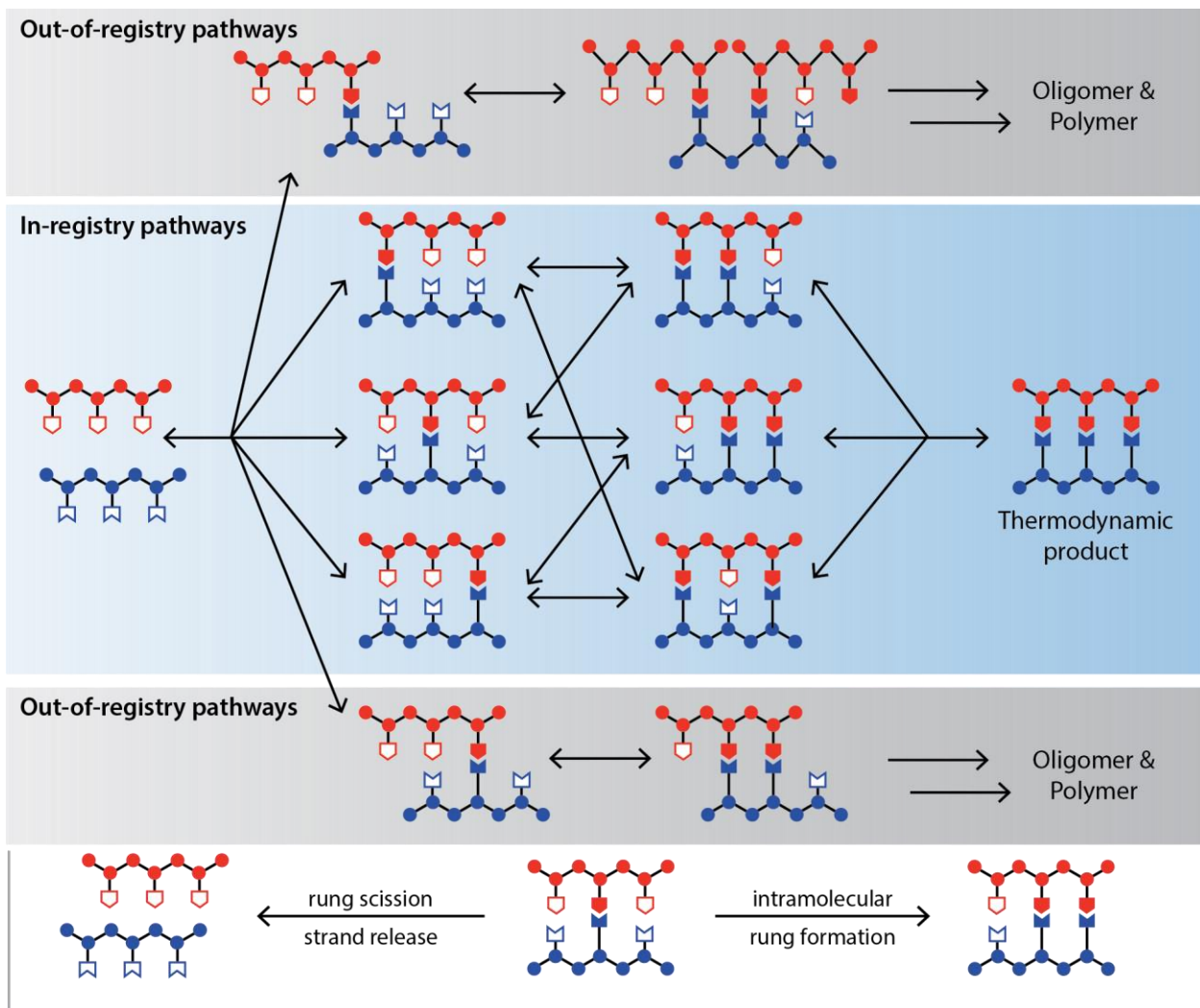
32 Most targets of DCC are constructed from a small number of different types of repeating  
33 units. Thus, DCC is commonly a **cyclooligomerization** process. The combination of a bimolecular  
34 oligomerization and intramolecular cyclization in the same reaction represents one challenge of  
35 dynamic covalent synthesis. Another challenge stems from the multtopic nature of DCC  
36 precursors. While the individual bond forming events are reversible, incorrectly joined structures  
37 may require multiple bond breakages to release an incorrectly placed precursor. Some erroneous  
38 structures fall out of **dynamic equilibrium** with the rest of the **reaction network**. This situation  
39 conjures up the notion of covalent bond **avidity**. Nonetheless, overcoming these challenges  
40 unleashes DCC's tremendous gain in synthetic efficiency reflected by the number of bonds made  
41 per operational step. Moreover, DCC product yields may approach quantitative, whereas  
42 cyclooligomerizations relying on strong irreversible bond formations tend to give low yields of  
43 final product, presumably because error correction is key to synthetic success [13].

44 Due to the reversibility of each bond forming event, DCC is generally thought to operate  
45 under **thermodynamic control**. The same literature survey mentioned above found that  
46 thermodynamic products and pathways are mentioned twice as much as kinetic products and  
47 pathways. However, as DCC advances to increasingly complex targets, there is good reason to  
48 suggest that kinetic factors may become more important. In this regard, there is an analogy between  
49 dynamic covalent synthesis and Levinthal's paradox for protein folding [14]. Levinthal's paradox  
50 states that because of the very large number of degrees of freedom in an unfolded polypeptide  
51 chain, the possible conformations are too vast to explore them all on the way to its native folded  
52 state. In a similar vein, the concatenation of multtopic precursors gives rise to a large number of  
53 structures on the way to the target product. These structures include polyhedra, polymers, and  
54 networks, and they may have very similar energies. This suggests a flat landscape, but complexes  
55 exhibiting covalent bond avidity are stabilized, which produces a vast landscape with somewhat  
56 regular variation. Given the complexity of DCC reaction networks and associated energy  
57 landscapes, synthetic intuition is unsuited to predict the outcome. Failures in experimental DCC  
58 often come at a high cost because multtopic, complex precursors require considerable structural

59 optimization and synthetic overhead [9]. Predicting outcomes is therefore essential and may  
60 require computational modeling to ensure a full understanding of the underlying factors that shape  
61 the energy landscape.

62 **Examples of Thermodynamically Controlled DCC**

63 The ability of dynamic systems to undergo reversible component exchange is key to the  
64 utility of DCC. Under thermodynamic control, even off-pathway intermediates typically error  
65 correct toward favorable product distributions on the timescale of the reaction (Figure 1) [15].  
66 Work from the Swager group recently demonstrated the reversibility of S<sub>N</sub>Ar in the synthesis of  
67 macrocycles and covalent organic frameworks from both free starting material and off-pathway  
68 kinetic intermediates [16]. Accessing the product distribution regardless of entry point into the  
69 reaction landscape is a necessary condition to classify the product distribution as a thermodynamic  
70 equilibrium. In a second example, arylene ethynylene macrocycles are formed both by alkyne  
71 metathesis cyclooligomerization and by depolymerization-macrocyclization of linear poly(arylene  
72 ethynylene) species [17].



73

74 **Figure 1.** Reaction network of ladder formation under DCC. In-registry intermediates and  
 75 products have correctly matched rungs where outer rungs bond to other outer rungs, and center  
 76 rungs bond to other center rungs between two strands. Out-of-registry products have mismatched  
 77 rung formation. Mismatched intermediates revert to free strands if rung scission is faster than  
 78 intramolecular rung formation.

79 Systems under thermodynamic control favor distributions that maximize entropy by  
 80 generating structures with the fewest possible number of building blocks while minimizing angle  
 81 strain of the resultant structures. These principles have enabled the intuitive design of a wide  
 82 variety of cyclic molecular architectures on the basis of precursor topicity and geometry [18].  
 83 Furthermore, in systems with very flat energy landscapes, slight differences in thermodynamic  
 84 stability lead to self-sorting and large amplifications of product concentrations, which can be

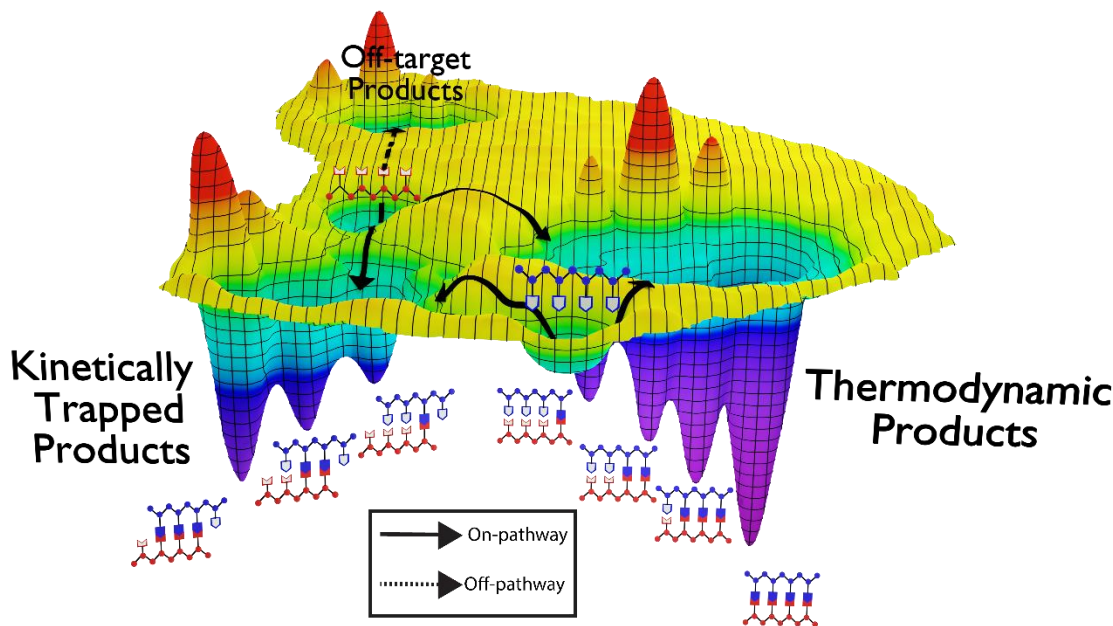
85 further improved by increased catalyst loading and thermal cycling [17,19-22]. The Cooper and  
86 Moore groups demonstrated that small energetic differences arising from chiral recognition are  
87 sufficient to direct the homochiral self-sorting of **dynamic covalent libraries (DCLs)** composed  
88 of racemic building blocks [19,23]. Zhang and coworkers recently demonstrated the synthesis of  
89 a cyclic porphyrin macrocycle via dynamic alkyne metathesis, which yielded the desired trimer in  
90 82% compared to a mixture of trimer (18%) and dimer (20%) via a kinetically controlled cross-  
91 coupling cyclooligomerization [24].

92 While design principles are generally reliable predictors of product topology and stability,  
93 occasionally this thinking belies the nuances of DCC energy landscapes. Cooper and coworkers  
94 recently designed a computational screening procedure to predict the outcomes of imine  
95 condensation reactions based on product stability [25]. While most combinations of aldehyde and  
96 amine precursors produced the predicted imine cages, several pairings of precursors led to  
97 structures with unexpected topologies. In these cases, the less thermodynamically favored product  
98 was observed, and the energetic preference for the predicted structures was determined to be small  
99 (around 5 kJ mol<sup>-1</sup>) compared to the observed products. The Zhang group reported similar  
100 phenomena in the synthesis of arylene ethynylene cages [26]. Slight variations in monomer size  
101 yielded structures with drastically different topologies, despite a consistent face-to-edge angle  
102 between substrates. Taken together, these results suggest that intuitive design rules are unreliable  
103 predictors of complex reaction outcomes, and that pathway-dependence may contribute to DCC  
104 syntheses in largely unexplored ways. Advancing DCC as a robust and reliable synthetic approach  
105 will likely benefit from extending the existing computational tools (*vide infra*).

## 106 Examples of Kinetically Controlled DCC

107 The reversible bonds used in DCC enable systems to undergo error correction. The faster the  
108 rate of exchange, the less prone the resulting system is to kinetic traps (Figure 2). A ladder with  
109 hydrogen bonded rungs demonstrates much higher fidelity (98% vs. 62%) than an imine-linked  
110 ladder with an identical backbone, due in part to the high exchange rate of hydrogen bonding  
111 [27,28]. However, while rapid exchange speed rescues a system from a putative kinetic trap, all  
112 covalent bonds are susceptible to trapping under some circumstances. Rigid complex architectures,  
113 such as COFs and cages, typically synthesized via DCC tend to be predisposed towards **kinetic**  
114 **control** due to precursor multtopicity. Macrocycles with ditopic precursors require two bond

115 breakage events before a precursor is released. After the first bond breakage, the two resulting  
116 reactive moieties are in close proximity and so have a faster rate of recombination than two  
117 unlinked precursors, an effect which is exacerbated by the rigidity of the structures. If the rate of  
118 bond reformation is faster than the breakage of the second bond, the macrocycle may behave as a  
119 kinetic trap. Kinetic trap behavior is even more likely for structures which require three or four  
120 bond breakages, where precursors are tritopic or tetratopic and the partially broken structures have  
121 higher rigidity [2,29]. This covalent bond avidity is apparent in the synthesis of ladder compounds,  
122 which generally have n-topic precursors, where n is the number of rungs. These studies show that  
123 beyond a certain number of rungs the structures can no longer undergo error correction and tend  
124 to form myriad mismatched products instead [8,30,31].



125  
126 **Figure 2.** In reactions with complex energy landscapes, species can become kinetically trapped  
127 even if reversible chemistry is used. Kinetic traps can persist if small barriers funnel material back  
128 to the trapped structure rather than out of the kinetic trap and toward a thermodynamic minimum.  
129 In the case of molecular ladders, out-of-registry products may be kinetic traps if rung scission is  
130 immediately followed by reformation of the rung. Kinetic factors such as proximity-induced high  
131 effective concentration prevent error correction in a dynamic system where the thermodynamic  
132 product is desired.

133 Rigidity also influences reaction outcomes by rendering certain transition states geometrically  
134 inaccessible. This is particularly relevant for reactions with conformationally restrictive transition  
135 states, such as the transition state leading to the metallocyclobutadiene intermediate in alkyne  
136 metathesis. Work in the Moore group to synthesize a molecular Möbius strip has demonstrated  
137 total kinetic diastereoselectivity because only one of the two possible diastereomeric intermediates  
138 could form the key metallocyclobutadiene transition state (Figure 3) [32].

139 Solubility is an ever-present consideration in the synthesis of complex architectures. Large  
140 structures common in DCC have decreased kinetic solubility. Heavily conjugated structures are  
141 common because they are rigid enough to be shape-persistent, but large, planar  $\pi$  surfaces  
142 contribute to insolubility due to  $\pi$ - $\pi$  stacking, removing the compound from dynamic equilibrium  
143 and promoting its formation. Dichtel and coworkers developed a system which produces  
144 macrocycle only when it is insoluble in the reaction solvent; dissolving the macrocycle and  
145 bringing it back into dynamic equilibrium leads to conversion into polymer, the putative  
146 thermodynamic product [1]. Many DCC syntheses are driven by precipitation [5,33-35]. Adding  
147 solubilizing groups or changing the size and planarity of the  $\pi$  surface allows modulation of  
148 solubility. Northrop and coworkers produce a planar and non-planar version of the same boronate  
149 ester cage by inserting ethynylene units into a biaryl backbone with a 90° twist [33]. They  
150 demonstrate that the more planar version is less soluble and more stable to protic solvents.

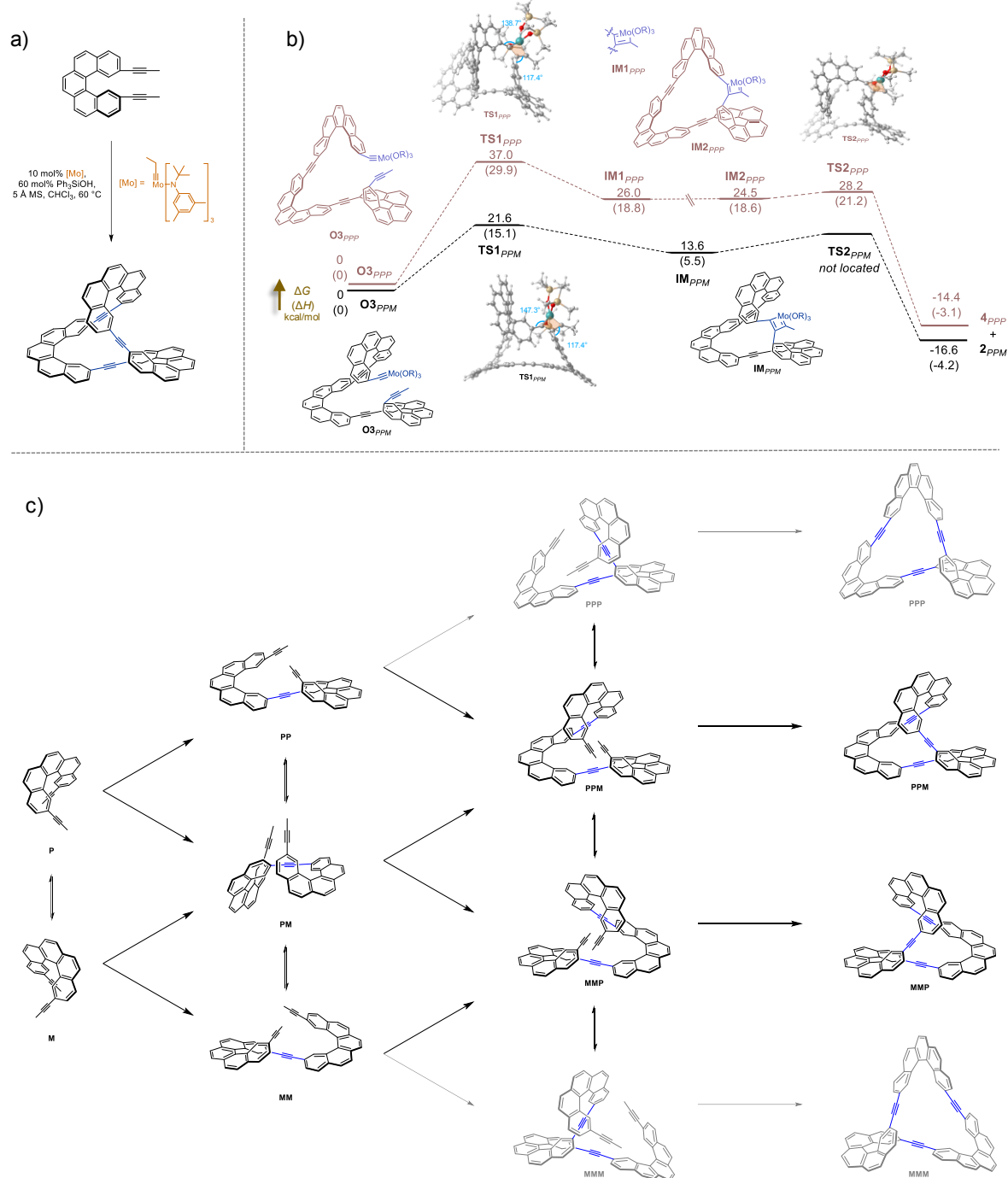


**Figure 3.** a) Alkyne metathesis of 2,13-bispropynyl helicene to form a C<sub>2</sub> symmetric molecular Möbius strip b) Energy profile demonstrating kinetic diastereoselectivity in macrocyclization c) reaction network showing intermediates leading to all possible stereoisomers. Structures in gray were not observed as products of the reaction.

152       **Supramolecular interactions** in solution also affect the product distribution in some  
153 systems. The enthalpic benefit of the interactions themselves drive the equilibrium toward  
154 compounds that promote more stabilizing supramolecular interactions.<sup>1</sup> In addition,  
155 supramolecular structures that form between cages and other complex products affect exchange  
156 rates. Dichtel and coworkers report an imine macrocycle that assembles into nanotubes which  
157 prevent further imine exchange, and Otto and coworkers report a similar effect [12,37]. In the  
158 synthesis of knots and catenanes from a DCL, multiple products are kinetically trapped as a result  
159 of intramolecular  $\pi$ - $\pi$  stacking in ambiphilic molecules, analogous to the hydrophobic effect in  
160 protein folding [38].

161       While kinetic traps may introduce synthetic obstacles, they sometimes provide products in  
162 higher yields than the same system under thermodynamic control (Box 1). In some cases, the  
163 kinetic trap is also the thermodynamic product [2,45]. In other cases, the pathway-dependence of  
164 kinetically controlled systems can be leveraged. Multiple products may be accessible from the  
165 same precursors under different conditions, especially useful given the high synthetic overhead of  
166 DCC precursors [12]. Otto and coworkers have provided evidence that mechanical agitation has a  
167 strong influence on product distribution [11,36]. Slow addition of monomer has been demonstrated  
168 to produce COFs with larger crystal domains than a single-addition protocol [46].

169       Kinetic control also allows improved information storage. Scott and coworkers show that a  
170 high-fidelity synthesis of an information-bearing five rung imine ladder is only achieved by  
171 increasing and then decreasing the concentration of scandium (III) triflate, commonly used to  
172 promote imine exchange [31]. This sort of chemical annealing is reminiscent of thermal annealing  
173 of DNA [31]. Keeping the concentration at the same low levels throughout the reaction leads to  
174 mismatched byproducts instead; this dependence on pathway suggests that the information-bearing  
175 ladders are kinetic products. Lehn and coworkers have developed libraries of acyl hydrazones and  
176 imines generated from simple aldehyde, acyl hydrazine, and aniline building blocks [8]. In the  
177 presence of metal cation with the appropriate coordination geometry, kinetically trapped species  
178 were favored. Upon precipitation of the directing metals, the libraries were expected to return to  
179 equilibrium, favoring formation of the more stable acyl hydrazone. However, because the  
180 exchange rate of imines and acyl hydrazones is on the order of weeks, the composition of the DCL  
181 remained unchanged on a relevant laboratory timescale, or until it was erased by thermal cycling.

182 Furthermore, the library could be trained to adopt an altered kinetic equilibrium through the  
183 addition of a different metal cation, demonstrating the versatility of a simple system for  
184 information storage. In this case, kinetic factors allow access not only to targeted materials, but  
185 also to emergent properties from simple chemical systems.

186 **Computational Studies**

187 Most efforts at rationally designing DCC systems have utilized thermodynamic modeling.  
188 Computational predictions of reaction outcomes based on thermodynamic driving forces have been  
189 used to design precursors and generally rely on the assumption that reactions will reach their  
190 thermodynamic end point (Box 2). The most common approach to thermodynamic modeling uses  
191 **DFT** to locate the energy of the various possible structures that could be formed in a given reaction  
192 network. The lowest energy structure is then assigned as the expected product. For DCLs, a  
193 common approach is to predict the equilibria in the library to understand the likely primary product  
194 and how that will change when reaction conditions are modified [47]. Thermodynamic modeling  
195 has also been widely used in designing molecular cages. The successful synthesis of a molecular  
196 cage by DCC requires precursors with the proper geometry. Cages designed by solely accounting  
197 for geometry have been moderately successful but some lack **permanent porosity** or fail to form  
198 [4,26]. The Cooper group has developed a **computational workflow** that accounts for both aspects  
199 [48]. Using this workflow combined with high throughput chemistry, they have synthesized a  
200 large number of unique cages [49]. However, their results still revealed unexpected cages as well  
201 as the failure of certain predicted cages to form at all[49,50]. While they attribute inconsistencies  
202 between theoretical and experimental results to entropy and solvent influences, it is likely that  
203 kinetic factors influenced the reaction outcome.

204 Kinetic modeling accounts for complex reaction networks and utilizes the rate coefficients  
205 for each reaction to predict the concentrations of species in the reaction. One technique for kinetic  
206 modeling involves manually calculating the reaction network and developing a master equation  
207 for all species in solution [51]. Another approach is to use **rule-based modeling** to state the rules  
208 of the reaction (e.g. changes in bonding or state) and to computationally generate the reaction  
209 network [29]. A third approach ignores the reaction network, and uses **Monte Carlo algorithms**  
210 to simulate the reaction [46,52,53]. Each of these approaches aims to predict the concentrations of  
211 all species in solution thus indicating key intermediates and the rate determining step [51], as well

212 as the presence of any kinetic traps [29]. Kinetic simulations provide guidance on optimal reaction  
213 conditions to increase the yield of the desired product [52]. Dichtel and coworkers recently utilized  
214 kinetic Monte Carlo simulations to better inform the synthesis of boronic ester covalent organic  
215 frameworks (COFs) [46,52,53]. Slow addition of monomer and inclusion of a competitive binder  
216 slowed growth and delayed nucleation, promoting controlled growth rather than uncontrolled  
217 nucleation of polycrystalline frameworks. These approaches yielded COFs with larger crystalline  
218 domains than structures synthesized via typical procedures, as well as larger diameters, greater  
219 uniformity of size, and higher signal to noise ratios in transient absorption and wide-angle x-ray  
220 scattering spectra.

221 **Conclusion**

222 While dynamic covalent chemistry is a relatively young field, consensus has already  
223 emerged around the importance of predicting reaction outcomes. Reversible covalent bonds  
224 combine the stability of covalent products with rapid error correction. However, not all linkages  
225 necessarily reversibly equilibrate and multitopicity of the resulting structures leads to complex  
226 reaction networks and energy landscapes. Unfortunately, the high overhead required to conceive  
227 of and develop precursors raises the cost of unpredictable outcomes [8]. Many researchers tend to  
228 overemphasize thermodynamic factors when planning a synthesis based on reversible covalent  
229 linkages even though the desired geometric complexity, rigidity, and extended conjugation often  
230 subject the synthesis to kinetic control. In response, computation has enhanced human intuition.  
231 New approaches have begun to incorporate kinetic factors into computation shedding light on COF  
232 nucleation, ladder formation and trapping, and other processes with observable kinetic effects  
233 [29,53]. However, few studies to date have incorporated both kinetic and thermodynamic factors  
234 in computational prediction.

235 We envision a future where computational models will be vital to developing new  
236 precursor structures. However, a new vision for a computational workflow which incorporates  
237 thermodynamic and kinetic considerations, and is accessible to organic and materials chemists, is  
238 sorely needed (Box 2). Developing and utilizing this new workflow will hopefully yield insights  
239 about unobservable intermediates and rate constants, and aid in our understanding of the  
240 fundamentals of DCC (outstanding questions). We hope that this will enable the synthesis of new  
241 complex and responsive materials and libraries.

242 **Box items**

243 **Box 1. Dynamic Systemic Resolution**

244 **Dynamic Resolution**

245 In many biological and synthetic systems, molecular recognition events are triggered by a  
246 slow, irreversible step which occurs due to a perturbation of a system previously under  
247 thermodynamic control. This perturbation occurs either through internal or external selection, and  
248 the resulting irreversible step removes kinetically trapped species from the dynamic pool, shifting  
249 equilibrium to favor their formation. This phenomenon, referred to as dynamic systemic resolution  
250 (DSR), is one way to combine the adaptive nature of thermodynamic control with the selectivity  
251 of kinetic control [10]. As an extension of classical dynamic kinetic resolution, this technique has  
252 been used for chiral resolution of epimers [40], as well as in biomimetic applications to amplify  
253 strong binders in the presence of receptor molecules [41].

254 Unlike thermodynamic DCC syntheses, the selectivity of DSR arises from reaction kinetics  
255 rather than product stability. Thus, the external kinetic stimulus must be chosen judiciously: it  
256 must be selective enough to operate quickly on the fastest-responding component of the DCL  
257 without directly affecting the rest of the DCL or halting the ongoing thermodynamic equilibrium  
258 [15]. Osowa and Miljanić used irreversible oxidation to enable self-sorting of a DCL of imines  
259 [42]. Slow oxidation of the imine species ensured that only the fastest-reacting amine and aldehyde  
260 pairs were removed from the dynamic pool, enabling highly efficient resolution of three discrete  
261 products from a library capable of producing nine different imines. Similar processes have been  
262 reported by Rizzuto and Nitschke in the synthesis of imine-based coordination cages [43].  
263 Antagonistic amplification of thermodynamically disfavored structures by kinetic requisition of  
264 more reactive imines resulted in the self-assembly of heteroleptic cages inaccessible by  
265 straightforward DCC synthesis. A major goal for DCC would be to use such DSR strategies to  
266 access and amplify kinetically trapped structures with low symmetry and unique functionality [44].

267 **Box 2. A computational workflow for synthetic design of DCC**

268 **Rational design** of DCC requires both thermodynamic and kinetic modeling and  
269 consideration. Solely considering either thermodynamic or kinetic impacts on DCC will not allow  
270 fully rational design, as both aspects influence DCC reactions. DCC needs a unified design

271 workflow that combines thermodynamic modeling for precursor design and kinetic modeling for  
272 conditions optimization while confirming that the desired product can actually be reached given  
273 the topicity of the precursor and kinetics of the type of DCC being used. The workflow should  
274 include initial thermodynamic modeling used to find likely candidates for the desired product,  
275 kinetic modeling to understand the reaction network leading to the predicted product, and possible  
276 thermodynamic redesign of the precursor if kinetic modeling shows there are many traps between  
277 precursor and product. The findings of the modeling are then applied to synthesis. We believe that  
278 this unified workflow is the future of DCC.

## 279 **Glossary Terms**

280 **Avidity:** A measure of total binding strength between multtopic components.

281 **Computational workflow:** A defined sequence of computational tasks that produce a desired outcome.

282 **Cyclooligomerization:** A reaction that converts monomers to macrocycles with a finite number of  
283 components.

284 **Density-functional theory (DFT):** A computational method used to model the electron density clouds of  
285 atoms and molecules in order to investigate their electronic and nuclear structure and predict their  
286 energies.

287 **Dynamic covalent chemistry (DCC):** A synthetic strategy typically utilizing reversible covalent bonds  
288 and multtopic precursors in order to synthesize networks, cages, and other architectures which would be  
289 difficult or impossible to synthesize in a stepwise manner.

290 **Dynamic covalent library:** Precursors designed to form a variety of different species via reversible  
291 covalent bonds are mixed to study the resulting product distribution and its response to perturbation.

292 **Dynamic equilibrium:** The concentration of all species is constant because the forward and reverse  
293 reactions are proceeding at equal rates. The system is at a thermodynamic minimum.

294 **Error correction:** The breakage of a bond which is incompatible with the system's intended product.  
295 This process is vital for the synthesis of complex architectures by DCC.

296 **Kinetic control:** The outcome of the reaction is primarily determined by which product is formed at the  
297 fastest rate and has the lowest activation energy of its formation, generally observed when the reaction is  
298 irreversible.

299 **Monte Carlo algorithms:** A type of computational algorithm which uses repeated random sampling and  
300 subsequent statistical analysis to obtain results for values which would otherwise be difficult to predict.

301 **Multitopic:** A precursor with multiple reactive sites which forms multiple bonds in the course of the  
302 reaction or synthesis.

303 **Permanent porosity:** Cavities are present in a molecule or material that do not collapse when the original  
304 hosts of the cavity (generally solvent molecules) are removed.

305 **Rational design:** The use of computer modeling to design a structure with specific desired properties,  
306 rather than using chemical intuition.

307 **Reaction network:** The total set of reactants, products, and intermediates in a system, and all the  
308 reactions that transform one into another.

309 **Reversible:** A reaction is reversible if the products react to reform starting material on a reasonable  
310 laboratory timescale.

311 **Rule-based modeling:** A model is defined by a set of rules repeatedly applied to progressive reaction  
312 conditions, allowing a complex model to be generated without specifying the system in its entirety.

313 **Supramolecular interactions:** Non-covalent interactions between molecules.

314 **Thermodynamic control:** The outcome of the reaction is primarily determined by which product is  
315 lowest in energy, generally observed when the reaction is reversible. Despite the rapid formation of the  
316 kinetic product, the thermodynamic product accumulates over time in a reversible reaction because the  
317 reverse reaction is slower for a more stable product.

318 **445 wrds**

## 319 **Acknowledgements**

320 This work was supported by the U.S. National Science Foundation (CHE-1904180) and the NSF  
321 GRFP (DGE-1746047) to S.D.L. The authors would like to thank Dorothy Loudermilk and Oleg  
322 Davydovich for assistance in making figures.

## 323 **Author Contributions**

324 <sup>†</sup>These authors contributed equally to this work.

## 325 **Notes**

326 The authors declare no competing financial interest.

327 **References**

- 328 1. Chavez, A. D. et al. (2018) Equilibration of imine-linked polymers to hexagonal macrocycles driven  
329 by self-assembly. *Chem. - A Eur. J.* 24, 3989–3993.
- 330 2. Lee, S. et al. (2016) Kinetically trapped tetrahedral cages via alkyne metathesis. *J. Am. Chem. Soc.*  
331 138, 2182–2185.
- 332 3. Niu, J. et al. (2018) Single-crystal x-ray diffraction structures of covalent organic frameworks.  
333 *Science* 52, 48–52.
- 334 4. Gasparini, G.; Dal Molin, M.; Lovato, A.; Prins, L. J. (2012) Dynamic Covalent Chemistry;  
335 *Supramolecular Chemistry: From Molecules to Nanomaterials*. (Gale, P. A., Steed, J.W. and  
336 Barbour, L.J., eds) John Wiley and Sons, Ltd.
- 337 5. The literature survey was completed by downloading all the unique articles found on SciFinder with  
338 the search term “dynamic covalent”. Once the non-searchable documents were removed, 1102 papers  
339 remained. These papers were text searched for various phrases using the command line tool ‘grep’. If  
340 a paper mentioned a specific structure (e.g. cage or polymer) ten or more times, it was considered to  
341 be the target structure. The specific percentages of target structures were: 55.4% polymer, 7.5%  
342 cages, 7.3% macrocycle, 4% dynamic covalent library, 3.5% covalent or metal-organic framework,  
343 1% ladder, 21.3% did not include any of these structures at least ten times. If a paper mentioned a  
344 specific chemistry ten or more times, it was considered to be the primary chemistry of the paper. The  
345 specific percentages of chemistries were: 22.5% imine, 14.0% boronic ester, 11.8% hydrazone  
346 exchange, 7.7% sulfide exchange, 4.3% metathesis (alkyne, olefin, or imine), 1.8% alkyne metathesis,  
347 1.7% oxime exchange, and 1.2% olefin metathesis.
- 348 6. Slater, A. G. et al. (2018) A solution-processable dissymmetric porous organic cage. *Mol. Syst. Des.*  
349 *Eng.* 3, 223–227.
- 350 7. Savino, C. et al. (2020) Electronic spectroscopy of 2-phenyl-1,3,2-benzodioxaborole and its  
351 derivatives: Important building blocks of covalent organic frameworks. *J. Phys. Chem. A* 124, 529–  
352 537.
- 353 8. Holub, J. et al. (2016) Training a constitutional dynamic network for effector recognition: Storage,  
354 recall, and erasing of information. *J. Am. Chem. Soc.* 138, 11783–11791.
- 355 9. Turcani, L. et al. (2019) Machine learning for organic cage property prediction. *Chem. Mater.* 31,  
356 714–727.
- 357 10. Herrmann, A. (2014) Dynamic combinatorial/covalent chemistry: a tool to read, generate and  
358 modulate the bioactivity of compounds and compound mixtures. *Chem. Soc. Rev.* 43, 1899–1933.

359 11. Evans, J. et al. (2017) Application of computational methods to the design and characterisation of  
360 porous molecular materials. *J. Chem. Soc. Rev.* 46, 3286–3301.

361 12. Pal, A. et al. (2015) Controlling the structure and length of self-synthesizing supramolecular polymers  
362 through nucleated growth and disassembly. *Angew. Chem. Int. Ed.* 54, 7852–7856.

363 13. Mastalerz, M. (2018) Porous shape-persistent organic cage compounds of different size, geometry,  
364 and function. *Acc. Chem. Res.* 51, 2411–2422.

365 14. Dill, K. A. and Chan, H. S. (1997) From Levinthal to pathways to funnels. *Nat. Struct. Biol.* 4, 10.

366 15. Zhang, W. and Jin, Y., eds (2017) *Principles of Dynamic Covalent Chemistry*; John Wiley & Sons,  
367 Ltd.

368 16. Ong, W. J. and Swager, T. M. (2018) Dynamic self-correcting nucleophilic aromatic substitution.  
369 *Nat. Chem.* 10, 1023–1030.

370 17. Gross, D. E.; Moore and Moore, J. S. (2011) Arylene–Ethynylene macrocycles via depolymerization–  
371 macrocyclization. *Macromolecules* 44, 3685–3687.

372 18. Moneypenny, T. P. et al. (2018) Product distribution from precursor bite angle cariation in multtopic  
373 alkyne metathesis: Evidence for a putative kinetic bottleneck. *J. Am. Chem. Soc.* 140, 5825–5833.

374 19. Sisco, S. W. and Moore, J. S. (2014) Homochiral self-sorting of BINOL macrocycles. *Chem. Sci.* 5,  
375 81–85.

376 20. Liu, X. and Warmuth, R. (2006) Solvent Effects in Thermodynamically Controlled Multicomponent  
377 Nanocage Syntheses. *J. Am. Chem. Soc.* 128, 14120–14127.

378 21. Wei, T. et al. (2017) Long, self-assembled molecular ladders by cooperative dynamic covalent  
379 reactions. *Polym. Chem.* 8, 520–527.

380 22. Elliott, E. L. et al. (2011) Covalent assembly of molecular ladders. *Chem. Commun.* 129, 4512-4513.

381 23. Greenaway, R. L. et al. (2019) From concept to crystals via prediction: Multi-component organic  
382 cage pots by social self-sorting. *Angew. Chem. Int. Ed.* 58, 16275–16281.

383 24. Yu, C. et al. (2016) Synthesis of cyclic porphyrin trimers through alkyne metathesis  
384 cyclooligomerization and their host-guest binding study. *Org. Lett.* 18, 2946–2949.

385 25. Greenaway, R. L. et al. (2018) High-throughput discovery of organic cages and catenanes using  
386 computational screening fused with robotic synthesis. *Nat. Commun.* 9, 2849.

387 26. Wang, Q. et al. (2016) Dynamic covalent synthesis of aryleneethynylene cages through alkyne  
388 metathesis: Dimer, tetramer, or interlocked complex? *Chem. Sci.* 7, 3370–3376.

389 27. Elliott, E. L. et al. (2011) Covalent ladder formation becomes kinetically trapped beyond four rungs.  
390 *Chem. Commun.* 47, 5028-5030.

391 28. Swain, J. A. et al. (2018) H-Bonded Duplexes based on a Phenylacetylene Backbone. *J. Am. Chem.*  
392 *Soc.* 140, 11526–11536.

393 29. Cencer, M. M. et al. (2020) Quantifying error correction through a rule-based model of strand escape  
394 from an  $n$ -rung ladder. *J. Am. Chem. Soc.* 142, 162–168.

395 30. Furgal, J. C. et al. (2019) . Accessing sequence specific hybrid peptoid oligomers with varied pendant  
396 group spacing. *Eur. Polym. J.* 118, 306–311.

397 31. Leguizamon, S. C. and Scott, T. F. (2020) Sequence-selective dynamic covalent assembly of  
398 information-bearing oligomers. *Nat. Commun.* 11, 1–10.

399 32. Jiang, X. and Laffoon, S. D. et al. (2020) Kinetic control in the synthesis of a Möbius  
400 tris((ethynyl)[5]helicene) macrocycle using alkyne metathesis. *J. Am. Chem. Soc.* 142, 6493–6498.

401 33. Smith, M. K. et al. (2015) The dynamic assembly of covalent organic polygons: Finding the optimal  
402 balance of solubility, functionality, and stability. *Eur. J. Org. Chem.* 13, 2928–2941.

403 34. Chavez, A. D. et al. (2016) Discrete, hexagonal boronate ester-linked macrocycles related to two-  
404 dimensional covalent organic frameworks. *Chem. Mater.* 28 (14), 4884–4888.

405 35. Ortiz, M. et al. (2017) Poly(aryleneethynylene)s: Properties, applications and synthesis through  
406 alkyne metathesis. *Topics Curr. Chem.* 375, 69.

407 36. Komáromy, D. et al. (2017) Self-assembly can direct dynamic covalent bond formation toward  
408 diversity or specificity. *J. Am. Chem. Soc.* 139, 6234–6241.

409 37. Strauss, M. J. et al. (2020) Supramolecular polymerization provides non-equilibrium product  
410 distributions of imine-linked macrocycles. *Chem. Sci.* 11, 1957–1963.

411 38. Ponnuswamy, N. et al. (2014) Homochiral and meso figure eight knots and a solomon link. *J. Am.*  
412 *Chem. Soc.* 136, 8243–8251.

413 39. Klotzbach, S. and Beuerle, F. (2015) Shape-controlled synthesis and self-sorting of covalent organic  
414 cage compounds. *Angew. Chem. Int. Ed.* 54, 10356–10360.

415 40. Simón, L. et al. (2010) Synthesis of a chiral artificial receptor with catalytic activity in michael  
416 additions and its chiral resolution by a new methodology. *Org. Biomol. Chem.* 8, 1763.

417 41. Larsson, R. et al. (2004) Catalytic self-screening of cholinesterase substrates from a dynamic  
418 combinatorial thioester library. *Angew. Chem. Int. Ed.* 43, 3716–3718.

419 42. Osowska, K. and Miljanić, O. Š. (2011) Oxidative kinetic self-sorting of a dynamic imine library. *J.*  
420 *Am. Chem. Soc.* 133, 724–727.

421 43. Rizzuto, F. J. and Nitschke, J. R. (2020) Narcissistic, integrative, and kinetic self-sorting within a  
422 system of coordination cages. *J. Am. Chem. Soc.* 142, 7749–7753.

423 44. Yan, Y. et al. (2016) Kinetic Trapping – a strategy for directing the self-assembly of unique  
424 functional nanostructures. *Chem. Commun.* 52, 11870–11884.

425 45. Castano, I. et al. (2019) Chemical Control over Nucleation and Anisotropic Growth of Two-  
426 Dimensional Covalent Organic Frameworks. *ACS Cent. Sci.* 5, 1892–1899.

427 46. Li, J. et al. (2014) Catenanes from catenanes: quantitative assessment of cooperativity in  
428 combinatorial catenation. *Chem. Sci.* 5, 4968-4974.

429 47. Berardo, E. et al. (2018) Computationally-inspired discovery of an unsymmetrical porous organic  
430 cage. *Nanoscale* 10, 22381-22388

431 48. Greenaway, R. L. et al. (2018) High-throughput discovery of organic cages and catenanes using  
432 computational screening fused with robotic synthesis. *Nat. Commun.* 9, 2849.

433 49. Greenaway, R. L. et al. (2019) From concept to crystals via prediction: multi-component organic cage  
434 pots by social self sorting. *Ang. Chem. Int. Ed.* 58, 16275-16281

435 50. Matsumura, Y. et al. (2017) A reaction model in the self-assembly process of octahedron shaped  
436 coordination capsules. *Phys. Chem. Chem. Phys.* 19, 20338-20342

437 51. Li, H. et al. (2020) Nucleation-elongation dynamics of two-dimensional covalent organic  
438 frameworks. *J. Am. Chem. Soc.* 142, 1367-1374

439 52. Li, H. et al. (2017) Nucleation and growth of covalent organic frameworks from solution: The  
440 example of COF-5. *J. Am. Chem. Soc.* 139, 16310–16318.

441 53. Evans, A. M. et al. (2018) Seeded growth of single-crystal two-dimensional covalent organic  
442 frameworks. *Science* 361, 52–57.

---